ORIGINAL PAPER

Semi-analytical approach to the determination of fracture permeability

Patrik Pusztai[1] 🄳 · Péter János Koroncz[2] · Máté Kuncz[2] · Anita Jobbik[1] · Ferenc Fedor[2]

Abstract

Proppant is one of the major elements of a hydraulic fracture process that can influence the productivity of an oil or gas well. The permeability of a propped fracture may be determined through laboratory measurements, utilizing experimental relationships, or using analytical methods. All methods have their advantages and disadvantages, and this study attempts to offers a solution that combines the various methods to achieve a practical solution. The standard measurement method for fracture conductivity and permeability is a time-consuming and delicate procedure and can be performed only at the cost of a significant degree of uncertainty. Investigating a method that can predict fracture permeability in significantly less time and with an acceptable level of accuracy would be useful for the industry. Proppant can be viewed as an unconsolidated, heterogeneous (in size distribution) although well-sorted granular packing, and the different relationships that can predict the permeability of such systems may be utilized. Such interdependencies account for the frictional pressure drop caused by the proppant particles and often neglect the pressure drop caused by the surface of the apparatus. To extend the applicability of the various models, the combination of a theoretical model that accounts for the pressure drop caused by the fracture wall with those models would have clear practical advantages. For this reason, a new equation had to be developed that establishes the relationship between the fracture permeability and the so-called modified particle friction factor. Since the frictional pressure drop correlations usually contain porosity as a parameter, determining its value under reservoir conditions is essential and a new procedure had to be developed. Since the different relationships were developed under different conditions to those under which

---

✉ Patrik Pusztai
   p.pusztai92@gmail.com

1 Research Institute of Applied Earth Sciences, University of Miskolc,
   Miskolc-Egyetemváros 3515, Hungary

2 Geochem Geological and Environmental Research, Consultancy and Service Ltd.,
   Kozármisleny 7761, Hungary

the proppant-packs are usually used, providing a solution to the issues of their wide range of application is the primary objective of this study.

1 Introduction

Hydraulic fracturing is a widely used stimulation technique in the oil and gas industry. The main objective is to create a highly conductive zone in the reservoir from which the liquid hydrocarbons can be produced at an economical rate (Mikelić et al. 2019). The fracture is usually prevented from closing by the application of a propping agent, the so-called proppant.

The determination of the fracture permeability of a propped fracture is a heavily investigated area of science, and the usual practice has been to make laboratory measurements (Kaufman et al. 2007; Guenaoui et al. 2022), or experimentally derive relationships (Berg 1970; Glover et al. 2006), or the use of analytical approaches (Lavrov 2017; Teng et al. 2020). Each of these methods has its advantages and disadvantages. The main objective of this study to establish a mathematical method which enables the combination of the different methods, thus reaping their benefits and creating a practical solution.

There are two different, widely accepted measurement methods in the industry for the determination of the fracture permeability and conductivity of proppant-packs. The first standardized measurement method was introduced by the American Petroleum Institute in 1989 under the code API RP 61, with the name "Recommended Practices for Evaluating Short Term Proppant-pack Conductivity" (API RP 61 1989). As this measurement method has a high degree of uncertainty, a modified approach and new equipment began to spread in the industry (Penny 1987). In the following years, this modified approach became the standard procedure in the industry, then the International Organization for Standardization adopted the method in 2008 under the code DIN EN ISO 13503-5 (ISO 13503-5 2006). Later, the American Petroleum Institute also adapted it under the code API RP 19D, and with the name "Recommended Practice for Measuring the Long-term Conductivity of Proppants" (API RP 19D 2008). It is worth mentioning that significant variances can be observed between measurements made under the same conditions. On average, the variance between the measurements is $\pm 20\%$, but variance as high as 80% also can be found (Richard et al. 2019; Anderson 2013). This phenomenon can be interpreted as being the result of various factors, but the main influencing factors on behavior is the proppant size distribution and the initial and loaded proppant arrangement, and in such cases, creating the same conditions is impractical (Liang et al. 2015). One can see that the API RP 19D measurement requires around two weeks to complete, which makes it impractical for the measurement of several samples for analysis.

The proppant can be viewed as an unconsolidated, heterogeneous (although well-sorted) granular packing, one of the main properties of which is the permeability that it can provide under reservoir conditions. The properties of flow through granular packings have been extensively studied over the past decades, both theoretically (Kozeny 1927; Carman 1937; Macdonald et al. 1979; Teng et al. 2020), numerically (Martys et al. 1994; Coelho et al. 1997; Zaman and Jalali 2010), and experimentally (Loudon 1952; Chapuis 2004; Erdim et al. 2015). The applicability of these models to the description of the permeability of propped fractures is limited. First, one of the main differences is that proppants are placed in reservoirs where the pressure and temperature ranges are higher than in the case of the studies mentioned above. These conditions can cause discrepancies in the models developed, as the granular materials are prone to deformation, crush, embedment, and corrosion, all of which represent challenges to the application of those models in such conditions (Schmidt and Steeb 2019). Second, most of the models do not take into account all the relevant mechanisms that can determine the propped fracture permeabilty. There are two driving mechanisms that have an impact on fracture permeability. One is the effect of viscous shear from the fracture wall, and the other is the viscous drag from the surface of the proppants (Brinkman 1949). It can be readily inferred that if the fracture is wider, then the viscous drag of the proppant will become more pronounced, and in the case of a narrower fracture or if the fracture is not propped efficiently, the effect of viscous shear on the wall becomes more pronounced. In most of the available theoretical models, the fracture permeability is approximated with the proppant-pack permeability (neglecting the effect of viscous shear from the wall), resulting in the fact thatmost of the models thus developed are inapplicable to scenarios in which the effect of viscous shear is considerable (Teng et al. 2020). Taking into consideration both mechanisms, there will be a transient zone in which the effect of both mechanisms is noticeable.

The permeability of an unpropped fracture, where only the viscous shear from the fracture wall is considered can be calculated by Eq. (1) proposed by Teng et al. (2020)

$$k_f = \frac{w_f{}^2}{12\mu} \tag{1}$$

where k_f is the fracture permeability, w_f is the fracture width, and μ is the dynamic viscosity of the fluid.

In order to visualize the effect in cases where only viscous drag is considered, an empirical relationship was used, as seen in Eq. (2) (Glover et al. 2006)

$$k_f = k_p = \frac{d_p{}^2 \phi_p{}^{3m}}{4am^2} \tag{2}$$

where k_p is the proppant-pack permeability, d_p is the geometric mean grain diameter, Φ_p is the porosity of the granular material pack, a is the dimensionless parameter that describes the sphericity of the granular material in the case of a 3D sample composed of quasispherical granular material its value is thought to be 8/3 (Schwartz et al. 1989), and m is the dimensionless cementation component, a value considered to be 1.5 in the case of spherical particles (Glover et al. 2006).
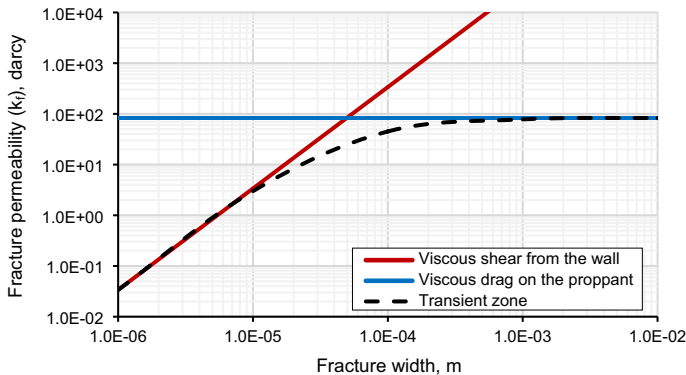
Fig. 1 Fracture permeability values using Eqs. (1), (2) (transient zone is just a visualization)

Using Eq. (1) to determine fracture permeability if only viscous shear is taken into account, and an empirical relationship, represented in Eq. (2), that considers only viscous drag from the proppant-pack, the two different mechanisms may be visualized as in Fig. 1, where the d_p, Φ_p, a, and m parameters in Eq. (2) are 0.4704 mm, 35%, 8/3, and 1.5, respectively. One can see that if only the viscous drag on the proppant is accounted for, then the fracture permeability remains constant regardless of the fracture width. If, in contrast, only the viscous shear on the fracture wall is considered, then the fracture permeability will be related to the square of the fracture width. This effect can also be readily inferred from Eq. (1). In reality, the effect of both mechanisms should be considered to effectively determine fracture permeability, thus a transient zone appears in certain dimensions (dashed line on Fig. 1) in which the viscous shear on fracture wall is more dominant at narrower fracture widths, and the viscous drag on the proppant particles is more pronounced at greater fracture widths.

Since several different models that consider only the viscous drag from the proppant-pack are available, one of the major objectives of this study is to develop an equation with which the applicability of the models can be extended to situations where the pressure drop on the apparatus wall cannot be neglected. Studies carried out specifically to determine the pressure drop on granular materials are the main focus of this study. In those models, one of the main parameters to be determined is the so-called frictional factor (or in a different form, the modified particle friction factor). Numerous correlations are available that can be used to identify the modified particle friction factor in the case of unconsolidated, heterogeneous granular packing. The limiting factors used in the course of the investigation are the Reynolds number ($Re = \frac{\rho d_p V}{\mu}$; where ρ is the fluid density, d_p is the average particle diameter, V is the fluid velocity based on the empty cross-section of the bed, μ is the fluid dynamic viscosity), modified Reynolds numbers ($Re_m = \frac{Re}{1-\Phi_p}$; $Re_1 = \frac{Re}{6(1-\Phi_p)}$; where Φ_p is the proppant-pack porosity), and porosity, valid under the measurement conditions. For comparison purposes, thirteen different relationships were selected, and the main equations with the applicable ranges are shown in Table 1.

Table 1 Modified particle friction factor relationships considered in this study

Author(s)	Modified friction factor	Equation	Applicable range
Carman (1937)	$f_\mathrm{p} = \left(180 + 2.871\left(\frac{Re}{1-\Phi_\mathrm{p}}\right)^{0.9}\right)\frac{(1-\Phi_\mathrm{p})^2}{\Phi_\mathrm{p}^3 Re}$	(3)	$0.01 < Re_1 < 10,000$
Rose (1945)	$f_\mathrm{p} = \left(\frac{1000}{Re} + \frac{60}{\sqrt{Re}} + 12\right)h(\Phi_\mathrm{p})$	(4)	$0.01 < Re < 10,000$ $0.32 < \Phi_p < 0.9$
Morcom (1946)	$f_\mathrm{p} = \left(\frac{784.8}{Re} + 13.73\right)\left(\frac{0.405}{\Phi_\mathrm{p}}\right)^3$	(5)	$Re < 750$
Rose and Rizk (1949)	$f_\mathrm{p} = \left(\frac{1000}{Re} + \frac{125}{\sqrt{Re}} + 14\right)h(\Phi_\mathrm{p})$	(6)	$0.01 < Re < 10,000$
Leva (1949)	$f_\mathrm{p} = 2f_\mathrm{m}\frac{(1-\Phi_\mathrm{p})^{(3-n)}}{\Phi_\mathrm{p}^3}$	(7)	$Re < 10,000$
Fahien and Schiver (1983)	$f_\mathrm{p} = \left(q\frac{f_{1L}}{Re_\mathrm{m}} + (1-q)\left(f_2 + \frac{f_{1T}}{Re_\mathrm{m}}\right)\right)\frac{(1-\Phi_\mathrm{p})}{\Phi_\mathrm{p}^3}$	(8)	*No data*
Tallmadge (1970)	$f_p = \left(150 + 4.2\left(\frac{Re}{1-\Phi_p}\right)^{5/6}\right)\frac{(1-\Phi_p)^2}{\Phi_p^3 Re}$	(9)	$0.1 < Re_m < 100,000$
Macdonald et al. (1979)	$f_p = \left(180 + 1.8\left(\frac{Re}{1-\Phi_p}\right)\right)\frac{(1-\Phi_p)^2}{\Phi_p^3 Re}$	(10)	$Re_m < 10,000$
Foscolo et al. (1983)	$f_p = (17.3 + 0.336Re)\frac{(1-\Phi_p)}{\Phi_p^{4.8} Re}$	(11)	*No data*
Meyer and Smith (1985)	$f_p = \left(90 + 0.462\left(\frac{Re}{1-\Phi_p}\right)\right)\frac{(1-\Phi_p)^2}{\Phi_p^{4.1} Re}$	(12)	$Re_1 < 1000$
Watanabe (1989); Kurten et al. (1966); Steinour (1944)	$f_p = 6.25\left(\frac{21}{Re} + \frac{6}{\sqrt{Re}} + 0.28\right)\frac{(1-\Phi_p)^2}{\Phi_p^3}$	(13)	$0.1 < Re < 4000$
Avontuur and Geldart (1996)	$f_p = \left(141 + 1.52\left(\frac{Re}{1-\Phi_p}\right)\right)\frac{(1-\Phi_p)^2}{\Phi_p^3 Re}$	(14)	$Re_m < 10,000$
Erdim et al. (2015)	$f_p = \left(160 + 2.81 Re_m^{0.904}\right)\frac{(1-\Phi_p)^2}{\Phi_p^3 Re}$	(15)	$2 < Re_m < 3600$

There is no literature that comprehensively analyzes and evaluates the applicability of different models for flow-through granular packings on proppant packings of different size distributions and under reservoir conditions. As all the models were developed not under usual reservoir conditions, a comprehensive analysis of its behavior is in the focus of our interest. On the basis of this analysis, a new model can be introduced which describes the fracture permeability under reservoir conditions more effectively.

Researchers also create analytical methods to evaluate fracture permeability using theoretical studies in order to eliminate the shortcomings of the empirical models.

Table 2 Advantages and disadvantages of the different method with which propped fracture permeability may be determined

	Advantages	Disadvantages
Measurement	Determines real behavior under reservoir conditions	High variances between measurements Long, delicate procedure
Experimental relationships	Easy to perform	Suitable under the conditions from which the relationships were derived Neglect the effect of viscous shear on the fracture wall
Analytical methods	Wider applicable range (than experimental models) Provide fast, stable and exact solutions Parameter dependencies are expressed explicitly	Proppant-pack permeability should be determined (by measurement or experimentally derived relationship) Reality often differs from ideal conditions

Analytical models are powerfull tools to describe flow through propped fractures, and are in the main focus of recent studies. Li et al. (2015) proposed an analytical model that considers proppant deformation and fracture aperture. Zhang et al. (2016) derived a theoretical model from the Berg (1970) correlation. In these models, the fracture permeability is approximated with the proppant-pack permeability, a reasonable step if the fracture is wide enough that the viscous shear on the fracture wall can be neglected. Teng et al. (2020) developed the first analytical model that considers not only the viscous drag on the proppant, but also the viscous shear on the fracture wall thus extending the applicable range of their model significantly. One major drawback of this model is that the proppant-pack permeability is still a compulsory input in their equation, and the determination of its value is nonetheless usually done on the basis of measurement or empirical correlations.

The main advantages and disadvantages of the different methods are collected in Table 2.

The purpose of this work is to find a solution in which the advantages of the different methods can be combined to synthesize a practical approach to determining the fracture permeability of a propped fracture. To achieve this, first an analytical solution was developed with which the relationship between the modified particle friction factor and the proppant-pack permeability was established. Then an analytical model that considers all the relevant mechanisms may be extended with the newly established relationship. As most of the models also require the proppant-pack porosities to be determined, a new measurement method had to be developed which enables the use of porosity values under reservoir conditions. Finally, testing and comparing the accuracy and the applicability of the new semi-analytical model was performed, and on the basis of the results an improved modified particle friction factor relationship was offered, describing the behavior of the granular material under reservoir conditions more accurately.

2 Methodology

2.1 Theoretical model

The literature contains a number of experimental relationships for calculating the pressure drop caused by fluid flow through packed beds. These interdependences can be utilized to determine the proppant-pack permeability. They are often accompanied by a so-called friction factor coefficient, which is a kind of descriptor of the viscous drag exerted by the granular packings (Erdim et al. 2015). This coefficient has been modified to the so-called "modified particle friction factor" seen in Eq. (16) (Montillet et al. 2007)

$$f_p = \frac{-\Delta P d_p}{\rho V^2 L} \tag{16}$$

where f_p is the modified particle friction factor, ΔP is the pressure difference between the inlet and the outlet, d_p is the particle mean diameter, ρ is the fluid density, V is the fluid velocity based on the empty cross-section of the bed, L is the length of the propped bed. This term is also often referred to as the "dimensionless pressure drop" (Eisfeld and Schnitzlein 2001).

The well-known Darcy's equation can be used to determine the permeability of a proppant-pack (Darcy 1856). The Darcy's equation shows a similarity to Eq. (16) and can be seen in Eq. (17).

$$V = \frac{-\Delta P k_p}{\mu L} \tag{17}$$

where μ is the dynamic viscosity of the fluid and k_p is the proppant-pack permeability. Combining Eq. (16) with (17) a relationship can be expressed that establishes the relationship between the proppant permeability and the modified particle friction factor.

$$f_p = \frac{d_p \mu}{\rho V k_p} \tag{18}$$

Utilizing the kinematic viscosity, the above equation can be modified as follows, in Eq. (19)

$$k_p = \frac{d_p \nu}{V f_p} \tag{19}$$

where ν is the kinematic viscosity of fluid. With Eq. (19) a compact, a new relationship is identified which establishes the connection between the proppant-pack permeability and the modified particle friction factor, thus enabling researchers to analyze the different models in cases of propped fractures.

Since a theoretical model that considers both the viscous shear and viscous drag should be used, Eq. (20) has been used (Teng et al. 2020)

$$k_f = k_p \left\{ 1 + \frac{2}{w_f} \left(\frac{v_o}{\frac{k_p}{\mu} \frac{\Delta P}{L}} + 1 \right) \sqrt{\frac{k_p}{\phi_p}} \left[csch\left(\sqrt{\frac{\phi_p}{k_p}} w_f \right) - coth\left(\sqrt{\frac{\phi_p}{k_p}} w_f \right) \right] \right\}$$

(20)

where k_f is the fracture permeability, w_f is the fracture width, v_o is the flow velocity at fracture walls (in case of laminar flow, the value is equal to 0), and Φ_p is the proppant-pack porosity. The term $csch$ gives the hyperbolic cosecant of the function, while the $coth$ gives the hyperbolic cotangent of the function. The model can be used under the following assumptions:

- The fluid is incompressible;
- The viscosity of the fluid is constant;
- The fluid flow is laminar and in a steady state;
- The effect of gravity is neglected;
- The proppants are immobile, and the porosity and permeability of the proppant-pack are constant.

Since the slippage on the fracture wall is assumed to be 0, as in the case of the measurements of laminar flow are performed Eq. (20) can be reduced to Eq. (21).

$$k_f = k_p \left\{ 1 + \frac{2}{w_f} \sqrt{\frac{k_p}{\phi_p}} \left[csch\left(\sqrt{\frac{\phi_p}{k_p}} w_f \right) - coth\left(\sqrt{\frac{\phi_p}{k_p}} w_f \right) \right] \right\}$$

(21)

Substituting Eq. (19) into (21) the different experimental relationships of modified particle friction factors can be analyzed. The final equation can be seen in Eq. (22).

$$k_f = \left(\frac{d_p v}{V f_p} \right) \left\{ 1 + \frac{2}{w_f} \sqrt{\frac{\left(\frac{d_p v}{V f_p} \right)}{\phi_p}} \left[csch\left(\sqrt{\frac{\phi_p}{\left(\frac{d_p v}{V f_p} \right)}} w_f \right) - coth\left(\sqrt{\frac{\phi_p}{\left(\frac{d_p v}{V f_p} \right)}} w_f \right) \right] \right\}$$

(22)

The driving parameters for determining the modified particle friction factors from Eq. 3 to 15 are the proppant-pack porosity and the Reynolds number (or a modified Reynolds number) valid in the case of porous media. As one model, namely Leva (Eq. 7), provided significantly higher fracture permeability values, it was eliminated. This can happen if the Reynolds number range during the measurements is lower than 11.5, which causes the value n in Eq. 7 to be equal to 1, and thus reduces the f_p value, consequently increasing the fracture permeability value of Eq. (22).

Testing the equations from Table 1 with the semi-analytical model developed here, the effect of the two driving mechanisms can be easily visualized, as seen in Fig. 2. With this method the applicability of the different modified particle friction factor
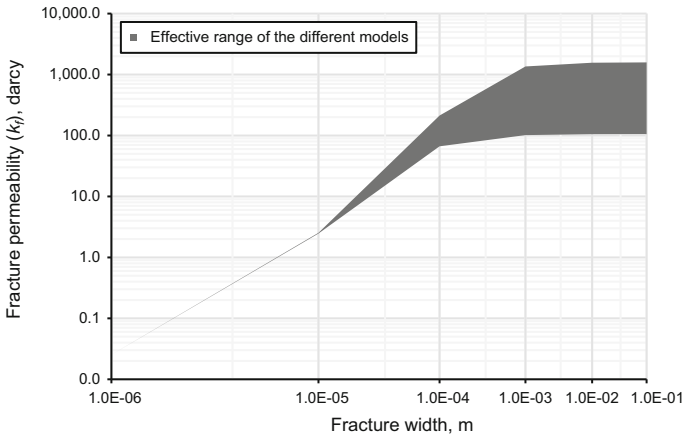
Fig. 2 Effective range of the different modified particle friction factor models using Eq. (22)

models was extended in those cases where the effect of viscous shear on the wall cannot be neglected.

It is evident that the final fracture permeability results are highly dependent on the modified particle friction model selected, as there is high variance. The two different zones dominated by the main mechanisms highlighted in Fig. 1 can be identified as well as the transient zone where the effect of the two mechanisms is equalized. In the case of a fracture width of 1–15 mm, as used by Aghili et al. (2019); Danko et al. (2020); Danko and Baracza (2022), the fluid flow can be mainly characterized by the viscous drag on the granular particles, while at a smaller width, such as 0.5 mm tested by Schmidt and Steeb (2019), the fluid flow is more affected by the viscous shear on the wall, and in the case of a 0.2 mm fracture width, as suggested by Bauer et al. (2016), the fluid flow is dominated by the viscous shear on the fracture wall (if the fracture is assumed to be filled with proppant particles).

2.2 Introduction of an extended, modified particle friction factor relationship

Since the modified particle friction factor relationships presented here do not take the effect of closing pressure into consideration, an extended relationship had to be developed to obtain better results. The correlation proposed by Foscolo et al. (1983) was used as a base. In our analyses, it is assumed that the closing pressure has an exponential effect on the proppant-pack because the particles under higher closure stresses can suffer more prominent deformation, breakage, and embedment. Modifying the model with an exponential closing pressure term, Eq. (23) was performed where P_c is the closing pressure in psi, α; a; b; and c are the correlation coefficients.

For the purposes of optimization, the genetic or evolutionary algorithm was selected, which incorporates randomness and inheritance into the optimization process (Wang et al. 2011), and is based on evolutionary computing, whose main idea takes Darwin's theory of evolution as its model/inspiration/basis (Kazemi et al. 2020). In essence,

the algorithm creates an analogy between the optimization process and the natural selection of living organisms. In an iterative process, the genetic search enhances a population of artificial individuals and the genetic information of the chromosomes (model variables) is randomly exchanged during the process (Szabó and Dobróka 2017). The steps of the optimization are illustrated in Fig. 3.

The main steps can be described as follows (Covas and Gaspar-Cunha 2009; Maad 2016): (1) The calculations start with the random definition of all the individuals composing the population (population initialization step). (2) In the following evaluation step, the values of the criteria for each individual are determined from the data created by the modeling routine. (3) Once these are known, it is possible to determine the fitness of every individual (value F). (4) This is then followed by the reproduction step, which is basically the cloning of an individual without modification to maintain high fitness in the next generation. (5) Then crossover of the selected individuals happens when the attributes of the parents are mixed. (6) The last basic operator is the mutation, which provides an element of randomness in the individuals of the population. (7) Calculations finish when all individuals converge on the same solution, or when a
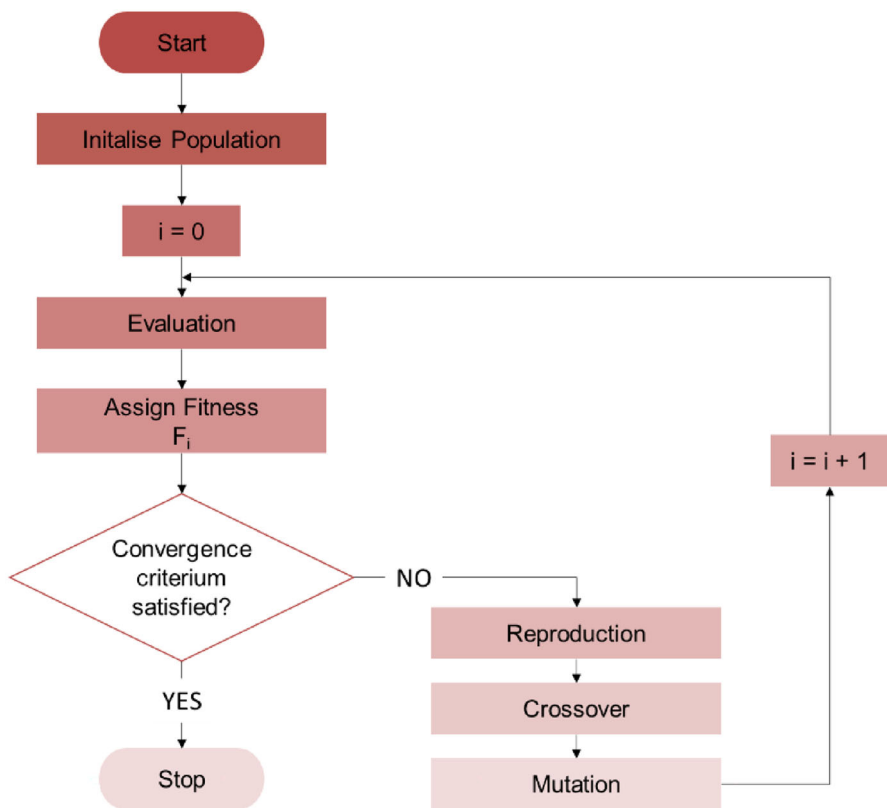
Fig. 3 Simplified flowchart of an evolutionary algorithm (Covas and Gaspar-Cunha 2009)

prescribed number of generations has been explored.

$$f_{\text{p}} = e^{\alpha \frac{P_c}{1,000}} \left[(a + b\text{Re}) \frac{(1 - \Phi_{\text{p}})}{\Phi_{\text{p}}^c \text{Re}} \right] \tag{23}$$

The objective of the optimization was to minimize the average gross variance of the calculated fracture permeability values to the measured values. After the optimization, Eq. (24) waswritten down.

$$f_{\text{p}} = e^{0.204 \frac{P_c}{1,000}} \left[(468 + 0.336\text{Re}) \frac{(1 - \Phi_{\text{p}})}{\Phi_{\text{p}}^{0.7} \text{Re}} \right] \tag{24}$$

Applying Eq. (24) to the developed semi-analytical model (Eq. (22)), the behavior of the models can be visualized under different closing pressures, as seen in Fig. 4.

The average values of the measured parameters were used with a constant flow velocity for Fig. 4. The effect of the two driving mechanisms can be easily identified. At higher closing pressures the effect of viscous drag on the proppant particles became more dominant at lower fracture widths than in the case of lower closing pressures. Also, with increasing closing pressure the final fracture permeability values decrease because the proppant particles suffer increasing deformations (crush, deformation, embedment, compaction, etc.). It can be seen that with different applied closing pressures on the proppant-pack, a difference with a magnitude can be reached.
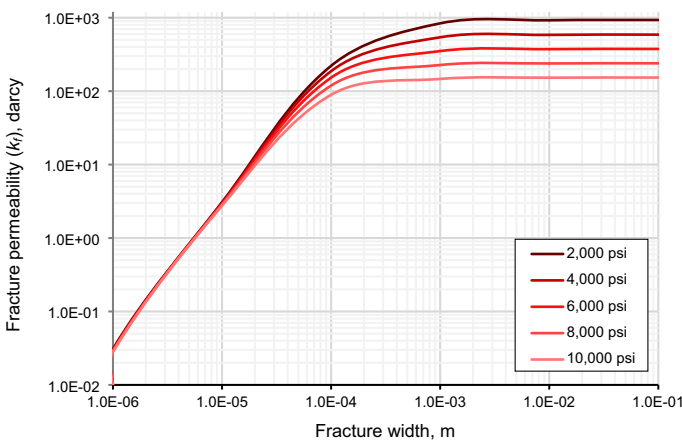
Fig. 4 Behavior of the new modified particle friction factor relationship in the case of a 30/50 mesh size proppant-pack under different closing pressures

3 Measurements

3.1 Permeability measurement

Based on the API RP 19D, eight measurements were performed on the standardized equipment on two different proppants and their different mass percentage mixtures to determine the proppant-pack permeabilities under different closing pressures. The proppants were spherical ceramic balls, but their size distribution and other parameters differed. This approach was chosen to determine the applicability of the models in a more comprehensive range of average proppant diameters by mixing the two types. The proppant with a smaller median particle diameter was a 30/50 mesh-sized lightweight ceramic proppant, while the proppant with the larger median particle size was a 16/32 mesh ceramic proppant with higher crush resistance.

Based on the API RP 19D, 6 measurements were performed to analyze the proppant-pack permeability under different applied closing pressures. To have a comprehensive dataset on proppant-packs with different average particle diameters, the two types of proppant were mixed by 20 m/m% increment. The results are illustrated in Fig. 5.

It can be seen from the above-presented results that the fracture permeability values decrease as closing pressure increase, and also decrease as average particle diameter decreases in the sample (a larger mass percentage of 30/50 mesh proppant in the mixture results in decreasing average median particle size). The connection between these variables is not linear, but rather exponential. It can be concluded from the results that a small amount of smaller diameter particles can have a significantly detrimental effect on the larger proppant's performance. In contrast, adding a small amount of larger proppant to a mixture cannot provide significantly better performance. This could also be inferred intuitively, as the smaller particles fill up the spaces between the larger particles, thus its permeability values will be dominant until there are not enough smaller particles to fill all the spaces between the larger particles. Also, as the closing
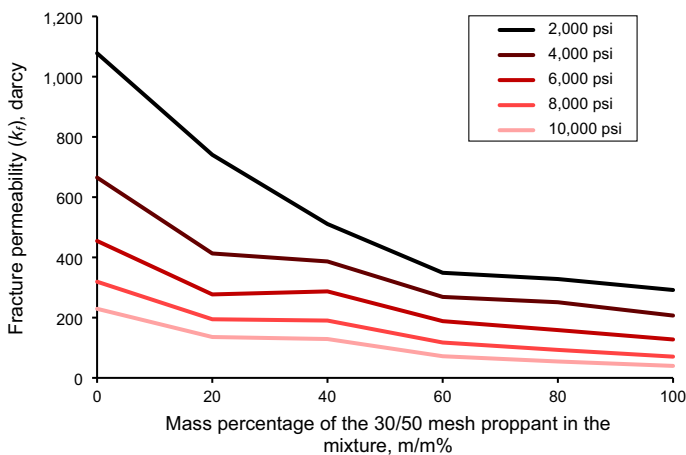

Fig. 5 Effect of mixing on permeability at different closing pressures

pressure becomes larger, the proppant-pack becomes more compact, thus providing smaller channels among the particles and increasing the tortuosity, so decreasing the permeability.

3.2 Porosity measurement

Using Eq. (22) and the modified particle friction factor relationships presented in Table 1, the measured fracture permeability values can be compared to the calculated results. As f_p equations contain the proppant-pack porosity (Φ_p) as a parameter, its values had to be determined. To calculate the porosity of the proppant-pack under different applied closing pressures, two parameters needed to be measured, which are the specific gravity of the proppant particle and the bulk density of the proppant-packs at each applied closing pressure.

The specific gravity measurements on the proppant-packs were performed at least three times, and the average gross variance between the measurements was 0.013%; this may be calculated using Eq. (25) provided by Richard et al. (2019), where σ is the standard deviation and $\overline{X}$ is the mean.

$$\text{Gross Variance} = \frac{\sigma}{\overline{X}} \tag{25}$$

A new method had to be developed to determine the bulk density of the proppant-pack under different applied closing pressures as no method can be found in the literature for this purpose. The crush test described in the API RP 19C (2008) was the basis of the bulk density measurement at different closing pressures. A schematic drawing of the measurement equipment is shown in Fig. 6.

Applying an exact mass of proppant in the cell and utilizing a width measurement device during the process described in the API RP 19C, the bulk densities can be easily calculated as the geometry of the cell and piston is well known, as in Eq. (26)

$$\rho_{bulk} = \frac{m_{prop}}{\left(\frac{d}{2}\right)^2 \pi h} \tag{26}$$

where ρ_{bulk} is the bulk density of the proppant-pack, m_{prop} is the mass of the proppant-pack in the cell, d is the diameter of the cell's inner side, h is the height of the proppant-pack. In the course of the measurements, the closing pressures were applied on the sample for two minutes (as described in the API RP 19C), and the proppant-pack widths were registered. Each measurement was performed three times, in order to be able to analyze the gross variance of the measurements. The average gross variance that was obtained by the measurements was 4.41%.

Since the specific gravities and bulk densities of the proppant-pack mixtures had been determined, the porosity of the proppant-pack under different closing pressures could then be calculated using Eq. (27)

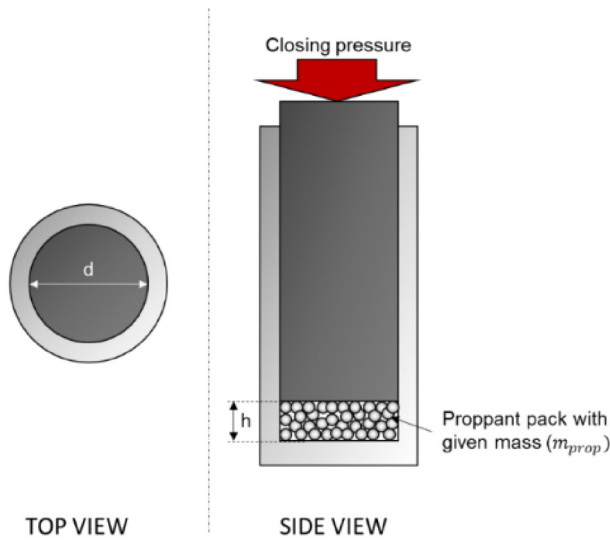$$\Phi_p = 1 - \frac{\rho_{bulk}}{\rho_{particle}} \tag{27}$$

Fig. 6 Schematic illustration of the crush test apparatus used during the bulk density measurements (not to scale)

where ρ_{bulk} is the measured bulk density of the proppant-pack at a given closing pressure in g/cm^3, and $\rho_{particle}$ is the particle density calculated from the specific gravity measurements in g/cm^3. The results can be seen in Fig. 7.

As the specific gravity of the proppant-pack decreases in a nearly linear manner with an increasing mass percentage of 30/50 mesh proppant in the mixture, and the bulk density follows a nearly parabolic decrease with an increasing amount of 30/50 mesh proppant in the mixture, the final porosity results show a decreasing trend until 20–30% of the 30/50 mesh proppant is in the mixture, and there is an increasing trend at higher concentrations.
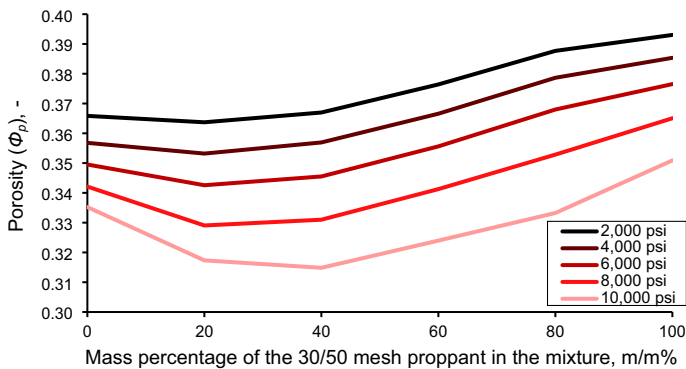
Fig. 7 Porosity values at different applied closing pressures in the case of different mixtures

4 Results

A relationship between the proppant-pack permeability and the modified particle friction factor has been established in the form of Eq. (19), which enables the testing of the different friction factor correlations (Table 1) in an analytical equation.

The analytical model provided by Teng et al. (2020) was complemented with the new relationship to extend the application range of the different correlations in cases in which the viscous shear on the fracture wall cannot be neglected.

A new measurement method was developed based on the API RP 19C standard measurement to determine the proppant-pack permeabilities under different closing pressures and thus provide sufficient input parameters to the different modified particle friction factor correlations. As far as the results go, the bulk density measurements can be reproduced with an average 4.4% gross variance.

The assessed modified particle friction factor correlations were tested with the new semi-analytical model. The results of the comparison can be seen in Fig. 6. On the basis of results, the calculated fracture permeability values did not match the measured values. After analyzing the results, an extended correlation was created in the form of Eq. (24), where the effect of closing pressure was considered. Comparing the new correlation with the measurements an average gross variance of 8.8% can be achieved, with a maximum value of 14.7%. The results are illustrated in Fig. 7. It can be seen that the calculated values do not perfectly match with the measurement results, since the porosity values slightly increased with the increasing mass percentage of larger proppant in the mixture (Fig. 8), while the fracture permeability values decreased (Fig. 5). Although the average 8.8% gross variance may not be practical in some applications, in the light of the relevant literature, it can be considered to be acceptable compared to the average gross variance yielded by the standard API fracture conductivity measurement.
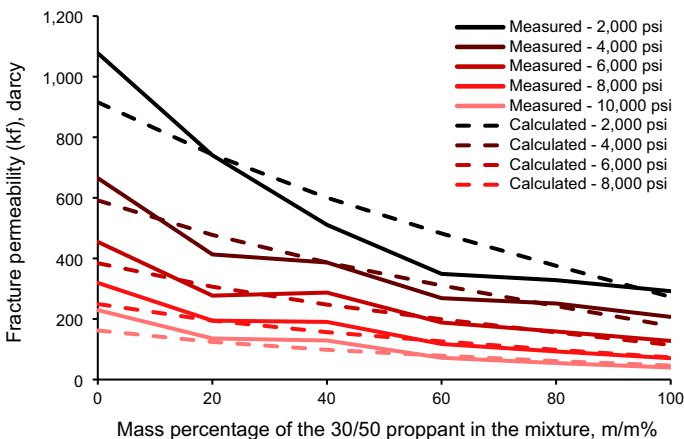

Fig. 8 Comparison of the present work to the measured fracture permeability values
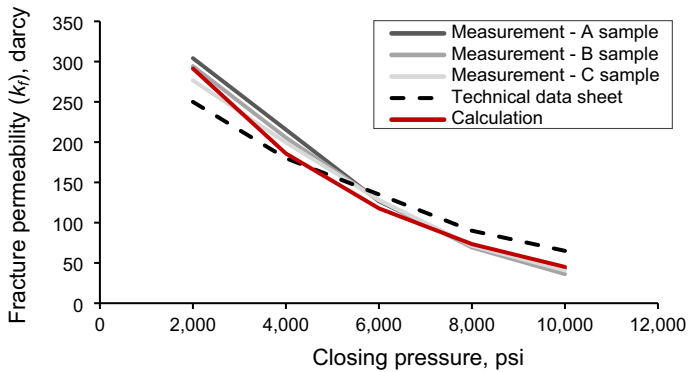
Fig. 9 Comparison of the measured and calculated fracture permeability values with the 30/50 mesh size proppant

The indicated 20% average gross variance of the API RP 19D standard measurement method can be considered significant, so it was important to determine what level of accuracy can be reached in our fracture permeability measurements. We performed the fracture permeability measurements 3 times on the 30/50 mesh size proppants, and the results are illustrated in Fig. 9. The results obtained show that the average gross variance between the measurements is significantly lower than reported in the literature, as its value is 3.9%. With this result, the reproducibility of the measurement was validated. Also, as the technical datasheet of this proppant was available, it was possible to compare the results to another independent laboratory's results. The fracture permeability values indicated in the technical datasheet imply slightly different results that measured in our work, with an average gross variance of 15.2%, which falls within the specified 20% range.

With the semi-analytical model developed, Eq. (22) and the new correlation, Eq. (24), the fracture permeability values calculated can be tested against the measured values (both to our measurements and to the technical datasheet). The calculated results had an average gross variance of 5.5% compared to our measurements, and 12.5% in the case of the technical datasheet. These results reinforced the validity of this new approach.

5 Discussion and conclusion

As oil and gas reserves are constantly decreasing, the role of intensification methods is growing in prominence. Transport and flow in fractured rock formations occur in several applications, such as enhanced oil and gas recovery, hydraulic fracturing, groundwater hydrology, etc. (Ambartsumyan et al. 2019). In the recent past, hydraulic fracturing treatment has become the focus of interest for several studies (Yoshioka et al. 2019). During this treatment usually, a granular propping agent is injected into the fracture that prevents the fracture from closure and thus provides a highly conductive zone for the fluid flow. As the hydraulic fracturing process is a complicated

and expensive technological process (Kushnir and Varypaev 2016), determining the permeability of the fracture and so the properties of the propping agent is essential. Understanding the behavior of the granular propping agent under reservoir conditions is a key objective of several studies. In this study, the utilization of the correlations on unconsolidated, granular materials and their applicability on proppant-packs under reservoir conditions were the main objectives.

A theoretical model was developed which considers both the viscous shear from the fracture wall and viscous drag from the surface of proppants and with which the behavior of the different modified particle friction factor correlations can be analyzed. One major result is the measurement process developed, with the aid of which the proppant-pack porosity can be measured under different closing pressures utilizing the API RP 19C crush test apparatus.

After the analyses, it was obvious that the assessed models could not be used efficiently to determine proppant behaviors under reservoir conditions. Since the porosity values of the proppant-pack under different closing pressures were determined, the comparison of the different models could be performed with the application of Eq. (22). The summary of the results is illustrated in Fig. 10. The average deviation from the measured values is represented by the maximum and minimum deviations. One can observe that the deviations are significantly higher than practicable (the practicable range can be considered within 20% variance, as Richard et al. (2019) showed).

Combining the investigated models represented in Table 1 with Eq. (22) as developed could not provide satisfactory results that might be considered useful. Some apparent facts can explain this result:

- In the case of the models represented in Table 1, the particles were unconsolidated, where the particles usually can move nearly freely, while in the course of the proppant measurements, the proppant particles were nearly in a fixed position.
- In the case of the models represented in Table 1, there was no pressure applied to the particles, while in the course of our measurements, the particles were under
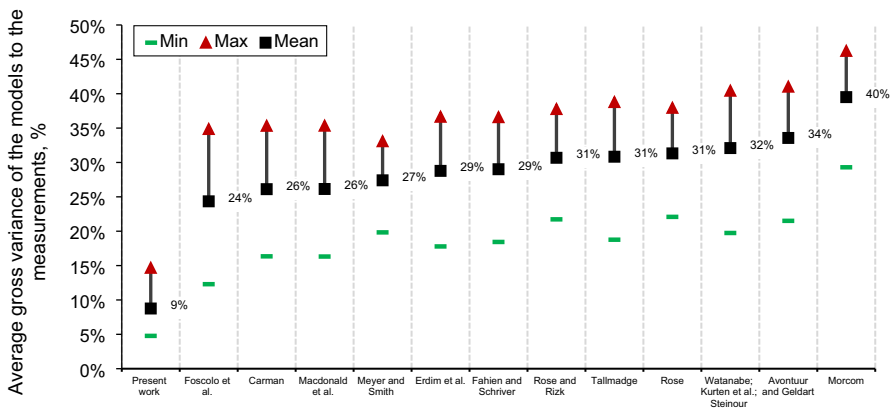

Fig. 10 Comparison of the calculated fracture permeability values to the measured values in the cases of the different models
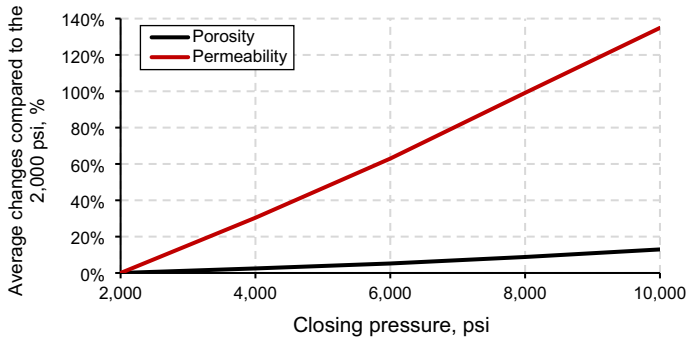
Fig. 11 Visualization of the effect of closing pressure on permeability and porosity

significant pressure, which can cause deformation, crushing, and embedment on the closure body's surface. These effects can have a significant negative effect on the final permeability results (Liang et al. 2016).

- Although pressure-dependent porosity values were measured, the final fracture permeability values could not predict the measurement values with sufficient accuracy. This phenomenon can be interpreted in the way that the stresses introduced by the closing pressure have a different effect on the permeability than on the porosities. Intuitively, if the proppant particles are deformed or rearranged, the porosities would not change significantly, while the free space for fluid flow between the particles changes significantly, resulting in an increasing tortuosity and so increasing fracture permeability. This aspect can be observed in Fig. 11, where the average changes compared to the 2000 psi closing pressures are visualized in the case of the measured fracture permeability and the measured porosity values. It can be seen that the change in permeability can be an order of magnitude larger than the change in porosity. This result confirms that the applied closing pressure has a higher effect on the permeability than on the porosity.

It can be readily inferred from these results that a correction is needed to the available models to overcome the effect of closing pressure. although pressure-dependent porosities were used (measured by the proposed new measurement method), the applied closing pressure has a higher effect on the permeability than on the porosity and the correlations used, which assume a relationship between the porosity and Reynold's number, cannot describe this effect efficiently. Although the final correlation, Eq. (24) does not perfectly fit the measured values, its applicability can be practical, as the API RP 19D standard measurement method can also be reproduced with nearly identical variances. The proposed method can predict the measurement results with an average gross variance of 8.8%.

One significant benefit of the proposed method is the less time required to obtain the permeability values than in the case of the standard measurement method. The API RP 19D measurement requires nearly two weeks to perform, while performing the proposed bulk density and specific gravity measurements on the samples only require around 1–2 h. This approach's benefit makes it practical and applicable to subsequent

research. It should be mentioned that the closing pressure-dependent term in Eq. (24) should be tested for different types of proppants in the future to ascertain the value of the coefficient over an even broader range.

Declarations

Conflict of interest The authors have declared that no competing interests exist.

Data availability Not applicable.

Code availability Not applicable.

References

Aghili, J., Brenner, K., Hennicker, J., et al.: Two-phase discrete fracture matrix models with linear and nonlinear transmission conditions. Int. J. Geomath. **10**(1), 24 (2019). https://doi.org/10.1007/s13137-019-0118-6

Ambartsumyan, I., Khattatov, E., Nguyen, T., et al.: Flow and transport in fractured poroelastic media. Int. J. Geomath. **10**, 11 (2019). https://doi.org/10.1007/s13137-019-0119-5

Anderson, R.: Performance of Fracturing Products. US Silica, Chandler, AZ (2013)

API RP 19C.: Measurement of Properties of Proppants Used in Hydraulic Fracturing and Gravel-packing Operations. 1st Edition, American Petroleum Institute (API) (2008)

API RP 19D.: Measuring the long-term conductivity of proppants. Washington, DC, API (2008)

API RP 61.: Recommended practices for evaluating short term proppant-pack conductivity. Washington, DC, API (1989)

Avontuur, P.P.C., Geldart, D.: A quality assessment of the Ergun equation. The 1996 IChemE Research Event/Second European Conference for Young Researchers1996, 994–996 (1996)

Bauer, M., Tóth, T.M., Raucsik, B., et al.: Petrology and paleokarst features of the Gomba hydrocarbon reservoir (central Hungary). Central Eur. Geol. **59**(1–4), 28–59 (2016). https://doi.org/10.1556/24.59.2016.003

Berg, R.R.: Method for determining permeability from reservoir rock properties. Gulf Coast Assoc. Geol. Soc. Trans. **20**, 303–317 (1970)

Brinkman, H.C.: A calculation of the viscous force exerted by a flowing fluid on a dense swarm of particles. Appl. Sci. Res. **A1**, 27–34 (1949). https://doi.org/10.1007/BF02120313

Carman, P.C.: Fluid flow through granular beds. Chem. Eng. Res. Des. **75**(Supplement), S32–S48 (1937). https://doi.org/10.1016/S0263-8762(97)80003-2

Chapuis, R.P.: Predicting the saturated hydraulic conductivity of sand and gravel using effective diameter and void ratio. Can. Geotech. J. **41**(5), 787–795 (2004). https://doi.org/10.1139/t04-022

Coelho, D., Thovert, J.-F., Adler, P.M.: Geometrical and transport properties of random packings of spheres and aspherical particles. Phys. Rev. E **55**(2), 1959–1978 (1997). https://doi.org/10.1103/PhysRevE.55.1959

Covas, J.A., Gaspar-Cunha, A.: Extrusion scale-up: an optimization-based methodology. Int. Polym. Process. **24**(1), 67–82 (2009). https://doi.org/10.3139/217.2200

Danko, G.L., Baracza, M.K.: Numerical demonstration of an unconventional EGS arrangement. Energies **15**(1), 20 (2022). https://doi.org/10.3390/en15010020

Danko, G., Jobbik, A., Baracza, M.K., et al.: Energy potential of a single-fracture, robust, engineered geothermal system. Geomech. Geophys. Geo-Energ. Geo-Resour. **6**, 26 (2020). https://doi.org/10.1007/s40948-020-00149-x

Darcy, H.: Les fontaines publiques de la ville de Dijon. Dalmont, Paris (1856)

Eisfeld, B., Schnitzlein, K.: The influence of confining walls on the pressure drop in packed beds. Chem. Eng. Sci. **56**, 4321–4329 (2001). https://doi.org/10.1016/S0009-2509(00)00533-9

Erdim, E., Akgiray, Ö., Demir, I.: A revisit of pressure drop-flow rate correlations for packed beds of spheres. Powder Technol. **283**, 488–504 (2015). https://doi.org/10.1016/j.powtec.2015.06.017

Fahien, R.W., Schriver, C.B.: Paper presented and Denver meeting of AlChE. In: Fahien, R.W. (ed.) Fundamentals of Transport Phenomena. McGraw-Hill, New York (1983)

Foscolo, P.U., Gibilaro, L.G., Waldram, A.: A unified model for particulate expansion of fluidised beds and flow in fixed porous media. Chem. Eng. Sci. **38**(8), 1251–1260 (1983). https://doi.org/10.1016/0009-2509(83)80045-1

Glover, P.W., Zadjali, I.I., Frew, K.A.: Permeability prediction from MICP and NMR data using an electrokinetic approach. Geophysics **71**(4), F49–F60 (2006). https://doi.org/10.1190/1.2216930

Guenaoui, A.S., Dobbi, A., Lebtahi, H., et al.: Experimental simulation of proppant permeability in hydraulic fracturing at extended time under bottom-hole conditions. J. Petrol. Explor. Prod. Technol. **12**, 1009–1021 (2022). https://doi.org/10.1007/s13202-021-01364-2

ISO 13503–5.: Procedures for measuring the long-term conductivity of proppants. Petroleum and natural gas industries – Completion fluids and materials – Part 5, Geneva, Switzerland, ISO (2006)

Kaufman PB, Anderson RW, Parker MA. et al.: Introducing new API/ISO procedures for proppant testing. SPE 110697, presented at 2007 SPE annual technical conference and exhibition, 11–14 November (2007) Doi: https://doi.org/10.2118/110697-MS

Kazemi, H., Yazdjerdi, K., Asadi, A., et al.: Application of genetic and K-means algorithms in clustering Babakoohi Anticline joints north of Shiraz. Iran, Central Eur. Geol. **63**(1), 38–48 (2020). https://doi.org/10.1556/24.2020.00004

Kozeny, J.: Ueber kapillare Leitung des Wassers im Boden. Sitzungsber Akad. Wiss. **136**(Abt. 2a), 271–306 (1927)

Kurten, H., Raasch, J., Rumpf, H.: Beschleunigung eines kugelförmigen Feststoffteilchens im Stromungsfeld konstanter Geschwindigkeit. Chem. Ing. Tech. **38**(9), 941–948 (1966). https://doi.org/10.1002/cite.330380905

Kushnir, A., Varypaev, A.: Accuracy of adaptive maximum likelihood algorithm for determination of micro earthquake source coordinates using surface array data in condition of strong coherent noise. Int. J. Geomath. **7**(2), 203–237 (2016). https://doi.org/10.1007/s13137-016-0082-3

Lavrov, A.: Fracture permeability under normal stress: a fully computational approach. J. Petrol. Explor. Prod. Technol. **7**, 181–194 (2017). https://doi.org/10.1007/s13202-016-0254-6

Leva, M.: Quoted in: Green DW, Perry RH. (Eds.), Perry's Chemical Engineering Handbook, 8 edn, Chemical Engineering, **56**, 115–117 (1949)

Li, K., Gao, Y., Lyu, Y., et al.: New mathematical models for calculating proppant embedment and fracture conductivity. SPE J. **20**, 496–507 (2015). https://doi.org/10.2118/155954-PA

Liang, F., Sayed, M., Al-Muntasheri, G.A., et al.: Overview of Existing Proppant Technologies and Challenges. Paper presented at the SPE Middle East Oil & Gas Show and Conference, Manama, Bahrain (2015).

Liang, F., Sayed, M., Al-Muntasheri, G.A., et al.: A comprehensive review on proppant technologies. Petroleum **2**(1), 26–39 (2016). https://doi.org/10.1016/j.petlm.2015.11.001

Loudon, A.G.: The computation of permeability from simple soil tests. Géotechnique **3**(4), 165–183 (1952). https://doi.org/10.1680/geot.1952.3.4.165

Maad, M.M.: Genetic algorithm optimization by natural selection. Comput. Sci. (2016). https://doi.org/10.13140/RG.2.2.23758.18246

Macdonald, L.F., El-Sayed, M.S., Mow, K., et al.: Flow through porous media-the Ergun equation revisited. Ind. Eng. Chem. Fundamen. **18**(3), 199–208 (1979). https://doi.org/10.1021/i160071a001

Martys, N.S., Torquato, S., Bentz, D.P.: Universal scaling of fluid permeability for sphere packings. Phys. Rev. E **50**(1), 403–408 (1994). https://doi.org/10.1103/physreve.50.403

Meyer, B.A., Smith, D.W.: Flow through porous media: comparison of consolidated and unconsolidated materials. Ind. Eng. Chem. Fundam. **24**(3), 360–368 (1985). https://doi.org/10.1021/i100019a013

Mikelić, A., Wheeler, M.F., Wick, T.: Phase-field modeling through iterative splitting of hydraulic fractures in a poroelastic medium. Int. J. Geomath. **10**, 2 (2019). https://doi.org/10.1007/s13137-019-0113-y

Montillet, A., Akkari, E., Comiti, J.: About a correlating equation for predicting pressure drops through packed beds of spheres in a large range of Reynolds numbers. Chem. Eng. Process. **46**(4), 329–333 (2007). https://doi.org/10.1016/j.cep.2006.07.002

Morcom, A.R.**:** Fluid flow through granular materials. Joint meeting of the Institution of Chemical Engineers with the Chemical Engineering Group, Apartments of the Geological Society, Burlington House, London, 30–43 (1946)

Penny, G.S.: An Evaluation of the effects of environmental conditions and fracturing fluids upon the long-term conductivity of proppants. Paper presented at the SPE Annual Technical Conference and Exhibition, Dallas, Texas (1987). Doi: https://doi.org/10.2118/16900-MS

Richard, S., Schrader, S., Schrader, R. et al.: Improved methods of measuring proppant conductivity. Paper presented at the SPE Western Regional Meeting, San Jose, California, USA (2019). Doi: https://doi.org/10.2118/195368-MS

Rose, H.E.: On the resistance coefficient–reynolds number relationship for fluid flow through a bed of granular material. ARCHIVE Proc. Inst. Mech. Eng. **153**, 154–168 (1945). https://doi.org/10.1243/PIME_PROC_1945_153_020_02

Rose, H.E., Rizk, A.M.A.: Further researches in fluid flow through beds of granular material. ARCHIVE Proc. Inst. Mech. Eng. **160**, 493–511 (1949). https://doi.org/10.1243/PIME_PROC_1949_160_047_02

Schmidt, P., Steeb, H.: Numerical aspects of hydro-mechanical coupling of fluid-filled fractures using hybrid-dimensional element formulations and non-conformal meshes. Int. J. Geomath. **10**, 14 (2019). https://doi.org/10.1007/s13137-019-0127-5

Schwartz, L.M., Sen, P.N., Johnson, D.L.: Influence of rough surfaces on electrolytic conduction in porous media. Phys. Rev. B Condens Matter. **40**(4), 2450–2458 (1989). https://doi.org/10.1103/physrevb.40.2450

Steinour, H.H.: Rate of sedimentation. Nonflocculated suspensions of uniform spheres. Ind. Eng. Chem. **36**(7), 618–624 (1944). https://doi.org/10.1021/ie50415a005

Szabó, N.P., Dobróka, M.: Exploratory factor analysis of wireline logs using a float-encoded genetic algorithm. Math. Geosci. **50**(3), 317–335 (2017). https://doi.org/10.1007/s11004-017-9714-x

Tallmadge, J.A.: Packed bed pressure drop – an extension to higher Reynolds numbers. AlChE J. **16**, 1092–1093 (1970). https://doi.org/10.1002/aic.690160639

Teng, B., Huazhou, L., Yu, H.: A novel analytical fracture-permeability model dependent on both fracture width and proppant-pack properties. SPE J. **25**(6), 3031–3050 (2020). https://doi.org/10.2118/201093-PA

Wang, Y., Cui, Y., Yang, C.: Hybrid regularization methods for seismic reflectivity inversion. Int. J. Geomath. **2**, 87–112 (2011). https://doi.org/10.1007/s13137-011-0014-1

Watanabe, H.: Drag coefficient and voidage function on fluid flow through granular packed beds. Int. J. Eng. Fluid Mech. **2**, 93–108 (1989)

Yoshioka, K., Parisio, F., Naumov, D., et al.: Comparative verification of discrete and smeared numerical approaches for the simulation of hydraulic fracturing. Int. J. Geomath. **10**, 13 (2019). https://doi.org/10.1007/s13137-019-0126-6

Zaman, E., Jalali, P.: On hydraulic permeability of random packs of monodisperse spheres: direct flow simulations versus correlations. Physica A **389**(2), 205–214 (2010). https://doi.org/10.1016/j.physa.2009.09.030

Zhang, J., Zhu, D., Hill, A.D.: Water-induced damage to propped-fracture conductivity in shale formations. SPE Prod. Oper. **31**, 147–156 (2016). https://doi.org/10.2118/173346-PA